Inorganic Chemistry

Article

Adamantane-like Cluster Complexes of Mixed-Valent Copper–Copper and Nickel–Copper Thiolates

**Matthew L. Miller,[†] Said A. Ibrahim,[‡] Melissa L. Golden,[†] and Marcetta Y. Darensbourg*,[†]**

Department of Chemistry, Texas A&M University, College Station, Texas 77845, and Department of Chemistry, Assiut University, Assiut, Egypt

Square-planar copper(II) and nickel(II) derivatives of the *cis*-dithiolate N_2S_2 ligand bis(N,N'-2-mercapto-2-methylpropyl)-1,5-diazocyclooctane, (bme*daco)M, nucleate four Cu^ICl moieties, forming $M^{II}_2Cu^I_4S_4$ clusters with unusual triply bridging thiolates, μ_3-SR, in the topological form of adamantane. As determined by X-ray crystallography, the (bme*daco)M (M = Cu or Ni) metallothiolate serves as a bidentate ligand that bridges four Cu^I ions, utilizing all lone pairs on sulfurs. Further characterization by electrochemical and electronic spectral measurements suggests greater electron delocalization in the all-copper complex as compared to the NiCu heterometallic complex. Mass spectral data imply that the mixed-metal $Ni^{II}_2Cu^I_4S_4$ is more stable toward CuCl loss than $Cu^{II}_2Cu^I_4S_4$, a result that is corroborated by extraction of Cu^I by 1,2-bis(diphenylphosphino)ethane in the latter but not the former.

Introduction

The well-known aggregative property of electron-rich sulfurs in metal-bound thiolates achieves a pinnacle of structural diversity with the late transition metals.[1] Copper thiolate aggregates can contain from 2 to 12 copper ions in a discrete unit, with cagelike structures ranging from tetrametallic to dodecametallic species.[1,2] Such clusters typically find sulfur-to-copper ratios equal to or greater than 1. In this way, the copper thiolate adamantane-like aggregate(s) isolated thus far contain four copper ions and six bridging thiolate ligands, e.g., $[Cu_4(SR)_6]^{2-}$ (R = Me, Et, Ph).[1,3] This results in three bonds to copper(I) ions and divalent, bridging sulfur sites, μ_2-SR. A stick drawing of $[Cu_4(SR)_6]^{2-}$, structure **A**, can be described as a tetrahedron of copper atoms that is edge-bridged by thiolate sulfur donors, i.e., producing an octahedron of S atoms inscribed onto a tetrahedron of Cu atoms. The alternate view, **A′**, shows the Cu—S connectivity in the perspective more typically associated with adamantane, $C_{10}H_{16}$, with four fused six-membered rings of Cu_3S_3. These constructions are both idealized and distortions exist.

S = SEt

A   A′
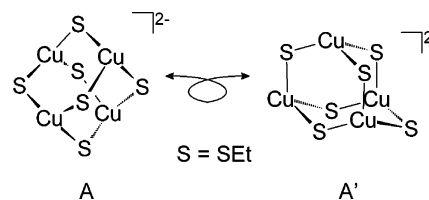
The reverse formulation, Cu_6S_4, is also a possibility for the same topological forms, because thiolates can act as triply bridging ligands. Such a mixed-valent $Cu^ICu^{II}(\mu_3$-SR) cluster was obtained in the work described below, initially by serendipity and later by design. The designed synthesis pointed to the possibility of an analogous heteronuclear complex $[Ni_2Cu_4]S_4$, which was also isolated and characterized by X-ray crystallography, mass spectrometry, electrochemistry, and electronic spectroscopy.

The bis-(N,N'-mercaptoethyl)-1,5-diazocyclooctane (bme-daco) ligand and its geminal dimethyl derivative, bis(N,N'-2-mercapto-2-methylpropyl)-1,5-diazocyclooctane (bme*daco), provide a N_2S_2 molecular matrix that readily accommodates square-planar geometry in its coordination complexes.[4] Despite its conformational constraints and steric bulk, the bme-daco ligand has been used to aggregate clusters involving up to five metals.[5] Shown in Chart 1 are examples of

---

* To whom correspondence should be addressed. E-mail: marcetta@mail.chem.tamu.edu.
  † Texas A&M University.
  ‡ Assiut University.
(1) Dance, I. G. *Polyhedron* **1986**, *5*, 1037−1104 and references therein.
(2) Janssen, M. D.; Grove, D. M.; Van Koten, G. *Prog. Inorg. Chem.* **1997**, *46*, 97−149.
(3) Dance, I. G.; Bowmaker, G. A.; Clark, G. R.; Seadon, J. K. *Polyhedron* **1983**, *2*, 1031−1043.

(4) (a) Mills, D. K.; Reibenspies, J. H.; Darensbourg, M. Y. *Inorg. Chem.* **1990**, *29*, 4364−4366. (b) Darensbourg, M. Y.; Font I.; Pala, M.; Reibenspies, J. H. *J. Coord. Chem.* **1994**, *32*, 39−49.
(5) Musie, G.; Farmer, P. J.; Tuntulani, T.; Reibenspies, J. H.; Darensbourg, M. Y. *Inorg. Chem.* **1996**, *35*, 2176−2183.


Chart 1

M = Ni, Pd
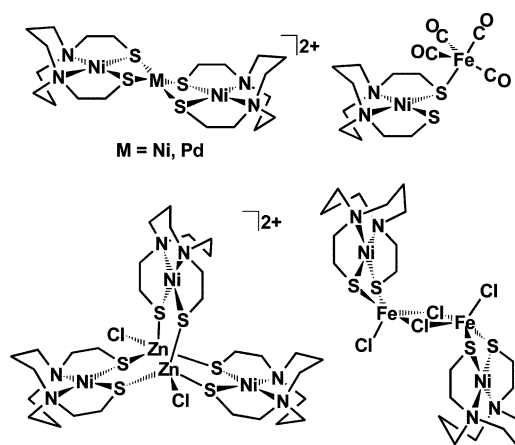
clusters based on (bme-daco)Ni as a metallothiolate ligand. A goal for this series was to determine the effect of the second metal on the redox potential of the nickel in the square-planar N_2S_2 environment.[5]

Additionally, nickel and iron aggregates were targets as synthetic models of the active site from nickel−iron hydrogenase, [NiFe]H_2ase, which contains two cysteine thiolate bridges between a nickel and an iron atom.[6,7] Of the most relevance to our current study is the pinwheel structure containing three nickel atoms and two zinc atoms.[8] This structure first demonstrated the bidentate, bridging capability of the metallodithiolate ligand.

Tolman and co-workers[9] developed copper analogues of (bme-daco)Ni as models for copper thiolate-containing enzyme sites. In that work, the monomeric (bme-daco)Cu was not isolated but appeared (in whole or in part) in various cluster forms. One example was a mixed-valent tri-copper(I,II,I) cluster shown as structure **B**.[9a]

B
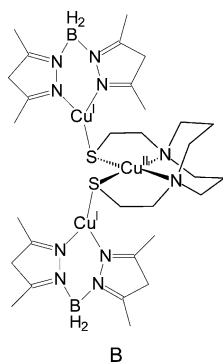
With a goal of managing the aggregative tendency of such N_2S_2Cu complexes, we have explored the use of the S-hindered bme*daco ligand and its complexes, (bme*daco)M (M = Cu, Ni), as metallothiolates for cluster formation. Herein, we report the synthesis and characterization of adamantane-like $M_2Cu_4S_4$ compounds, which, to our knowledge, are the first of their kind. During the preparation of

this manuscript, Schugar and co-workers reported an extensive electronic spectroscopic study of mixed-valent Cu^{II}−Cu^I aggregates with up to five copper atoms based on a related cis-N_2S_2 ligand whose monomeric Cu^{II} complex building block is shown as structure **C**.[10]

C

∠N−Cu−N	84.6°
S−Cu−S	106.6°
N_2Cu / S_2Cu	32.8°
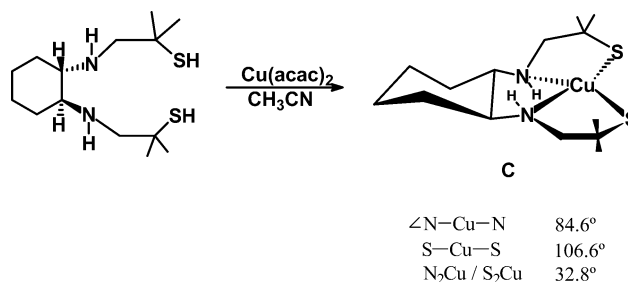
Experimental Section

General Techniques. All syntheses and manipulations of materials were carried out under an argon atmosphere using Schlenk techniques or a glovebox. Solvents were dried under a dinitrogen atmosphere prior to use according to published procedures.[11] Methanol or acetonitrile solvents were further purged with a stream of argon and stored over 3A molecular sieves. Cu(acac)$_2$ (acac = acetylacetonate) (Lancaster Synthesis Inc.) and CuCl (Aldrich Chemical Co.) were used as received. N,N'-Bis(2-mercapto-2-methylpropyl)diazocyclooctane (H$_2$bme*daco) and its nickel complex, (bme*daco)Ni, were synthesized according to published procedures.[12]

Physical Methods. Vis/UV spectra were recorded on a Hewlett-Packard HP8452A diode array spectrophotometer. Elemental analyses were performed by Canadian Microanalytical Systems in Delta, British Columbia, Canada.

^{1}H NMR spectra, for use in determining magnetic susceptibility via the Evan's method,[13] were obtained from acetonitrile solutions on a Mercury-300 FT-NMR spectrometer. Electrospray ionization mass spectrometry data were obtained at the Laboratory for Biological Mass Spectrometry, Texas A&M University, College Station, Texas, using an MDS Series Qstar Pulsar with a spray voltage of 5 keV. EPR spectra were obtained from 0.2 mM ethanol glasses at 8 K using a Bruker EMX spectrometer operating at 9.453 GHz and 0.2 mW of power.

Cyclic voltammograms were obtained on a BioAnalytical Systems 100A electrochemical analyzer equipped with three electrodes: a glassy carbon working electrode, a platinum wire auxiliary electrode, and a Ag/AgNO$_3$ reference electrode. Measurements in CH$_3$CN were either 1.13 or 2.25 mM in analyte and 0.1

(6) Volbeda, A.; Garcin, E.; Piras, C.; de Lacey, A. L.; Fernandez, V. M.; Hactchikian, E. C.; Frey, M.; Fontecilla-Camps, J. C. *J. Am. Chem. Soc.* **1996**, *118*, 12989−12996.

(7) Lai, C.-H.; Reibenspies, J. H.; Darensbourg, M. Y. *Angew. Chem., Int. Ed. Engl.* **1996**, *35*, 2390−2393.

(8) Tuntulani, T.; Reibenspies, J. H.; Farmer, P. J.; Darensbourg, M. Y. *Inorg. Chem.* **1992**, *31*, 3497−3499.

(9) (a) Houser, R. P.; Tolman, W. B. *Inorg. Chem.* **1995**, *34*, 1632−1633. (b) Houser, R. P.; Young, V. G., Jr.; Tolman, W. B. *J. Am. Chem. Soc.* **1996**, *118*, 2101−2102.

(10) Stibrany, R. T.; Fikar, R.; Brader, M.; Potenza, M. N.; Potenza, J. A.; Schugar, H. J. *Inorg. Chem.* **2002**, *41*, 5203−5215.

(11) Gordon, A. J.; Ford, R. A. *The Chemist's Companion*; Wiley and Sons: New York, 1972; pp 430−437.

(12) Mills, D. K.; Font, I.; Farmer, P. J.; Tuntulani, T.; Buonomo, R. M.; Goodman , D. C.; Musie, G.; Grapperhaus, C. A.; Maguire, M. J.; Lai, C.-H.; Hatley, M. L.; Smee, J. J.; Bellefuille, J. A.; Darensbourg, M. Y. *Inorg. Synth.* **1998**, *32*, 89−98.

(13) (a) Evans, D. F. *J. Chem. Soc.* **1959**, 2003−2005. (b) Sur, S. K. *J. Magn. Reson.* **1989**, *82*, 169−173. (c) Grant, D. *J. Chem. Educ.* **1995**, *72*, 39−40.

M in [n-Bu$_4$N](PF$_6$) (TBAHFP) as the supporting electrolyte. All potentials were scaled to NHE using Cp$_2$Fe/Cp$_2$Fe$^+$ (referenced to +400 mV in CH$_3$CN according to the literature[14]) as the standard. Measurements were performed at room temperature under a nitrogen atmosphere.

**Preparations. (bme*daco)Cu.** Typically, 0.29 g (1.0 mmol) of H$_2$bme*daco dissolved in 5 mL of THF was added to a slurry of 0.13 g (0.50 mmol) of Cu(acac)$_2$ in 10 mL of THF. The light blue Cu(acac)$_2$ solution immediately changed to a dark blood-red color. After ca. 5 min, (bme*daco)Cu began to precipitate, and 30 mL of pentane was added to afford almost complete precipitation as a microcrystalline metallic orange powder. This powder was collected on a glass frit under anaerobic conditions, washed with pentane (3 × 10 mL), and then dried under vacuum. Yields varied according to the purity of the ligand and ranged from 0.072 g (41%) to 0.134 g [76% based on Cu(acac)$_2$]. Red platelike crystals were obtained upon slow diffusion of pentane vapor into THF solutions of (bme*daco)Cu. Anal. Calcd (found) for C$_{14}$H$_{28}$CuN$_2$S$_2$: C, 47.8 (47.4); H, 8.02 (8.15); N, 7.96 (7.96). Vis/UV in acetonitrile solution: λ_{max} (ϵ, M^{-1} cm^{-1}): 198 (9500), 352 (7000), and 504 (590).

{[(bme*daco)Cu]$_2$(μ-CuCl)$_4$} (Cu$_6$S$_4$adam). Typically, 0.100 g (0.28 mmol) of (bme*daco)Cu was dissolved in 20 mL of acetonitrile and added to a slurry of 0.085 g (0.86 mmol) of CuCl in 10 mL of acetonitrile. Dark red-black crystals suitable for X-ray crystallographic studies were grown from diffusion of ether into an acetonitrile solution of the reaction mixture. Yield: 0.052−0.078 g [33−50% based on (bme*daco)Cu. Anal. Calcd (found) for C$_{28}$H$_{56}$Cl$_4$Cu$_6$N$_4$S$_4$·0.5CH$_3$CN·0.5(C$_2$H$_5$)$_2$O: C, 32.2 (30.8); H, 5.44 (5.30); N, 5.44 (4.75). Vis/UV in acetonitrile solution: λ_{max} (ϵ): 206 (36 000) and 454 (6300).

{[(bme*daco)Ni]$_2$(μ-CuCl)$_4$} (Ni$_2$Cu$_4$S$_4$adam). A 0.109 g (0.31-mmol) portion of (bme*daco)Ni[12] was dissolved in 20 mL of acetonitrile and added to a slurry of 0.085 g (0.86 mmol) of CuCl in 10 mL of acetonitrile. The solution was layered with ether, and the resulting orange-red precipitate was recrystallized in a 1:1:1 mixture of methanol/acetonitrile/ether. Yield: 0.164 g [84% based on (bme*daco)Ni]. Crystals suitable for X-ray crystallographic studies were grown from slow diffusion of ether into a methanol/acetonitrile solution. Anal. Calcd (found) for C$_{28}$H$_{56}$Cl$_4$Cu$_4$N$_4$Ni$_2$S$_4$·1.5CH$_3$OH: C, 31.1 (31.4); H, 5.49 (5.25); N, 4.92 (4.89). Vis/UV in 1:1 methanol/acetonitrile λ_{max} (ϵ): 234 (41 000). ^{1}H NMR (CD$_3$CN/CD$_3$OD 50:50): 3.49 q (8H), 2.82 s (8H), 2.63 m (8H), 1.69 s (24H), 1.19 t (8H).

X-ray Structure Determinations. X-ray data were obtained on a Bruker Smart 1000 (Cu$_6$S$_4$adam and Ni$_2$Cu$_4$S$_4$adam) or an Apex CCD (Cu$_5$S$_4$adam′) diffractometer and covered a hemisphere of space upon the combination of three sets of exposures. The space groups were determined on the basis of systematic absences and intensity statistics.[15] The structures were solved by direct methods. Anisotropic displacement parameters were determined for all non-hydrogen atoms. Hydrogen atoms were added at idealized positions and refined with fixed isotropic displacement parameters equal to 1.2 (1.5 for methyl protons) times the isotropic displacement parameters of the atoms to which they were attached. Atoms that proved to be non-positive-definite were corrected by including the command ISOR with the "s" parameter set at 0.05 in the instruction file. Programs used include SMART[15] for data collection and cell

Scheme 1
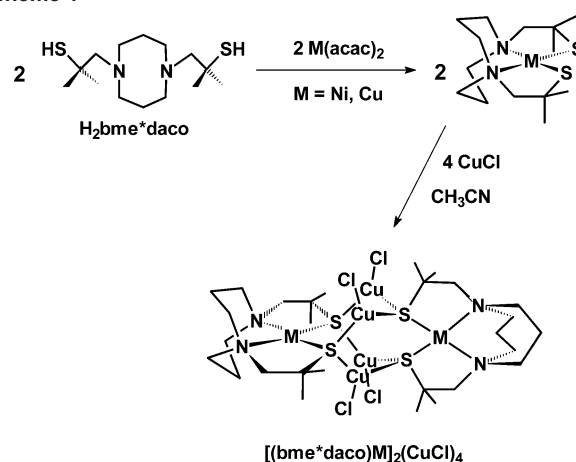
refinement, SAINT-Plus[16] for data reduction, SHELXS-86 (Sheldrick)[17] for structure solution, SHELXL-97 (Sheldrick)[18] for structure refinement, and SHELXTL-Plus, version 5.1 or later (Bruker)[19] for molecular graphics and preparation of material for publication.

Results and Discussion

Synthesis. Scheme 1 displays the two-step synthesis of the new cluster complexes. Similarly to the preparation of (bme*daco)Ni,[12] Cu(acac)$_2$ reacted with the H$_2$bme*daco dithiol in THF to produce a dark red solution from which the N$_2$S$_2$Cu monomer precipitated. The red platelike crystals that were obtained from a tetrahydrofuran/pentane mixture proved unsuitable for X-ray crystallographic analysis.

The red-black solid resulting from the (bme*daco)Cu/2CuCl reaction is soluble in acetonitrile and methanol and insoluble in diethyl ether. The deep purple acetonitrile solution of (bme*daco)Ni changed to orange-red upon reaction with 2 equiv of CuCl, yielding an orange precipitate. The nickel−copper cluster complex is soluble in a 50:50 mixture of acetonitrile and methanol but only slightly soluble in the individual pure solvents; it is insoluble in diethyl ether.

Characterization in the Solid State. Despite differences in solubility, the Cu−Cu and the Ni−Cu complexes have the same formulation, [(bme*daco)M]$_2$(μ-CuCl)$_4$, Cu$_6$S$_4$adam, and Ni$_2$Cu$_4$S$_4$adam; they crystallize in the same monoclinic crystal system and space group, $P2_1$. Both solids include solvent molecules of crystallization, and both have two independent molecules within their asymmetric units. Crystallographic data and collection parameters for Cu$_6$S$_4$adam and Ni$_2$Cu$_4$S$_4$adam are given in Table 1. (The isolation of the copper-deficient, adamantane-like cluster, Cu$_5$S$_4$adam′, is described later.) Full structural reports are available in the Supporting Information, along with extended packing diagrams. The latter show, for Cu$_6$S$_4$adam·0.5MeCN·0.5OEt$_2$,

(14) Gagne, R. R.; Koval, C. A.; Lisensky, G. C. *Inorg. Chem.* **1980**, *19*, 2854−2855.

(15) *SMART 1000 CCD*; Bruker Analytical X-ray Systems: Madison, WI, 1999.

(16) SAINT-Plus, version 6.02 or later; Bruker Analytical X-ray Systems: Madison, WI, 1999.

(17) Sheldrick, G. *SHELXS-86: Program for Crystal Structure Solution*; Institüt für Anorganische Chemie der Universität: Göttingen, Germany, 1986.

(18) Sheldrick, G. *SHELXL-97: Program for Crystal Structure Refinement*; Institüt für Anorganische Chemie der Universität: Göttingen, Germany, 1997.

(19) *SHELXTL*, version 5.1 or later; Bruker Analytical X-ray Systems: Madison, WI, 1998.

Table 1. Crystallographic Data[a] for the Adamantane-like Complexes

	Cu₆S₄adam	Ni₂Cu₄S₄adam	Cu₅S₄adam′
formula	$C_{28}H_{56}Cl_4Cu_6N_4S_4 \cdot$ 0.5MeCN·0.5Et₂O	$C_{28}H_{56}Cl_4Cu_4N_4Ni_2S_4 \cdot$ 1.5MeOH	$C_{28}H_{56}Cl_3Cu_5N_4S_4 \cdot$ 3MeCN
formula weight	1151.08	1136.44	1124.22
temperature (°C)	−163.15	−163.15	−173.15
wavelength (Å)	0.710 73	0.710 73	0.710 73
Z	4	4	4
D_{calcd} (g/cm³)	1.614	1.615	1.607
μ (cm⁻¹)	30.76	30.12	26.37
crystal system	monoclinic	monoclinic	monoclinic
space group	$P2_1$	$P2_1$	$P2_1/n$
unit cell			
a (Å)	11.516(2)	11.427(2)	10.800(2)
b (Å)	19.117(4)	19.027(4)	39.376(7)
c (Å)	21.765(4)	21.759(4)	11.773(2)
β (°)	98.754(5)	98.842(4)	111.886(3)
volume (Å³)	4736.0(16)	4674.7(16)	4645.8(14)
GOF	0.935	0.969	0.880
R_1^b, wR_2^c(%) [$I > 2\sigma(I)$]	6.11, 14.82	7.09, 16.57	4.58, 8.80
R_1^b, wR_2^c(%) all data	8.64, 15.94	9.45, 17.52	8.35, 11.93

[a] Obtained using graphite-monochromatized Mo Kα radiation ($\lambda = 0.710\ 73$ Å) at 110K. [b] $R_1 = \Sigma||F_o| - |F_c||/\Sigma F_o$. [c] $wR_2 = [\Sigma[w(F_o^2 - F_c^2)^2]/\Sigma w(F_o^2)^2]^{1/2}$.
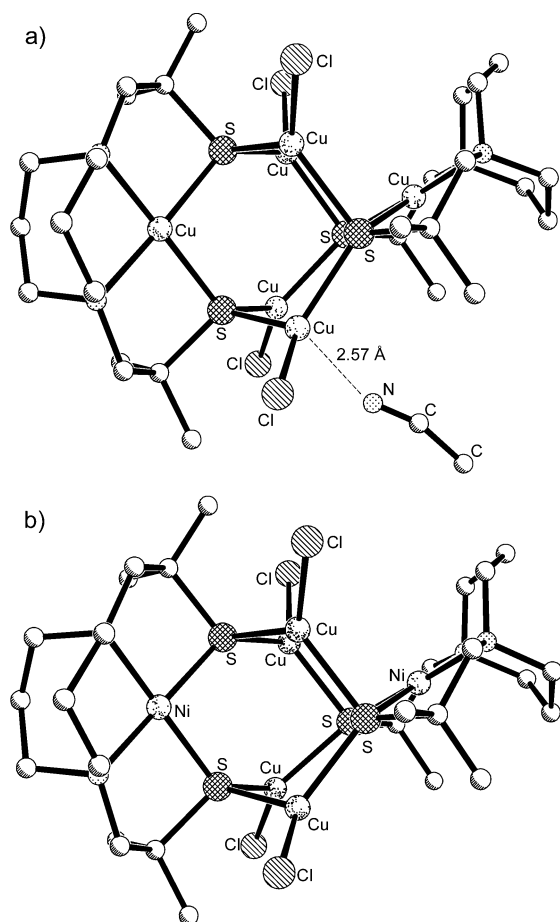
Figure 1. Ball-and-stick representations of the molecular structures of (a) Cu₆S₄adam with selected atoms labeled and (b) Ni₂Cu₄S₄adam. Hydrogen atoms are omitted.

a long-range (2.57 Å) interaction of the acetonitrile solvent with one CuᴵCl in 50% of the molecules, whereas Ni₂Cu₄S₄adam·1.5MeOH has no specific solvent−metal ion interactions.

The molecular structures of Cu₆S₄adam and Ni₂Cu₄S₄adam are shown in Figure 1a and b, respectively; selected average bond distances and angles are listed in Table 2. Numbers in

Table 2. Selected Average Bond Distances and Angles and Averaged Uncertainties for Cu₆S₄adam, Ni₂Cu₄S₄adam, and Cu₅S₄adam′

	Cu₆S₄adam	Ni₂Cu₄S₄adam	Cu₅S₄adam′
Mᴵᴵ−N (Å)[a]	2.06(2)	1.99(2)	2.06(2)
Mᴵᴵ−S (Å)[a]	2.26(1)	2.17(1)	2.258(9)
Cuᴵ−S (Å)	2.24(1)	2.23(1)	2.235(8)
Cuᴵ−Cl (Å)	2.192(9)	2.199(7)	2.22(2)
N−M−N (°)[a]	89.9(4)	91.2(8)	89.1(3)
S−M−S (°)[a]	94.9(6)	91.6(4)	93.7(2)
S−M−N (°)[a]	87.6(5)	88.6(5)	89(1)
Cl−Cuᴵ−S (°)	125(4)	124(4)	124(6)
S−Cuᴵ−S (°)	108(2)	110(2)	113(6)
Cuᴵ−S−Mᵃ (°) small[b]	97(4)	99(4)	94(4)
Cuᴵ−S−Mᵃ (°) large[b]	130(3)	134(2)	130(2)
Cuᴵ−S−Cuᴵ (°)	104(5)	98(5)	102(8)
N₂S₂ vs Cu₂S₂ (°) small[c]	95(1)	97(2)	93(1)
N₂S₂ vs Cu₂S₂ (°) large[c]	161(2)	165(2)	166(6)

[a] M = Cu in Cu₆S₄adam and Cu₅S₄adam′; M = Ni in Ni₂Cu₄S₄adam. [b] Small defines the Cuᴵ−S−M unit in the more open face of the N₂S₂M unit, whereas large derives from the Cuᴵ−S−M unit in the opposite face. [c] Similarly to footnote b, small is that dihedral angle between the Cu₂S₂ plane and the more open N₂S₂ plane; large is the opposite, sterically hindered N₂S₂ face.

parentheses following each value are standard uncertainties in the specific values averaged over from 4 to 16 individual M−L distances. The molecular structures reveal that the complexes are constructed of two N₂S₂M (M = Cu, Ni) monomers bridged by four CuCl moieties. The divalent metals are in the square-planar cavity of the N₂S₂ ligands. Each sulfur atom is further bound to two copper(I) atoms, one above and one below the N₂S₂M plane, achieving a distorted tetrahedral geometry, surrounded by a carbon, Mᴵᴵ, and two Cuᴵ ions. The N₂S₂M units are in roughly perpendicular planes; the angle between the planes is ca. 110°. As was found in monomeric (bme*daco)Ni,[4b] the 2-mercapto-2-methylpropyl arms of the bme*daco ligand are in an eclipsed conformation in both of the complexes, and the fused metallodiazacyclohexane rings are in a boat/chair conformation.

Figure 2 contains ball-and-stick representations showing the coordination about the divalent metal ions in Cu₆S₄adam and Ni₂Cu₄S₄adam. The mean deviation from planarity in the CuN₂S₂ unit is 0.0151 Å and in NiN₂S₂, 0.0132 Å;
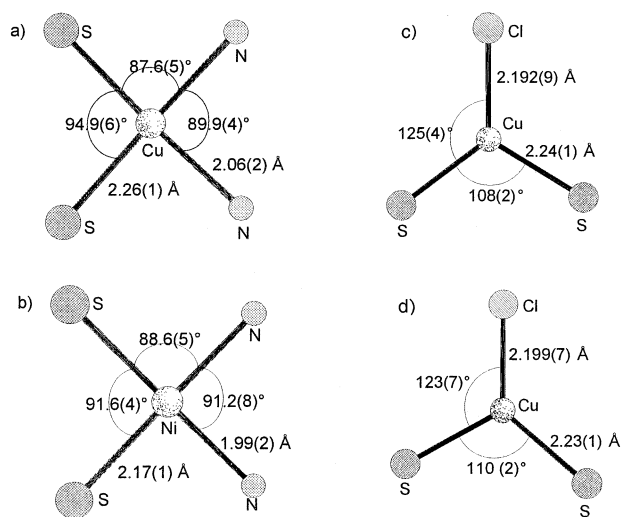
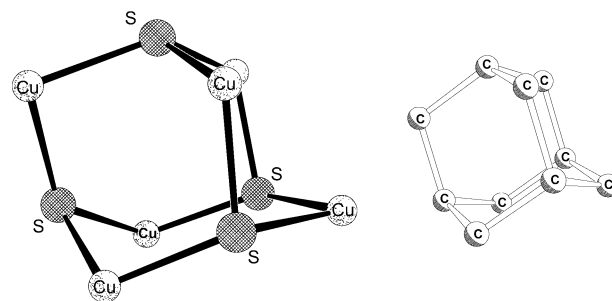**Figure 2.** Ball and stick representations isolating the coordination of (a) Cu^{II} in Cu_6S_4adam; (a′) Cu^I in Cu_6S_4adam; (b) Ni^{II} in $Ni_2Cu_4S_4$adam; (b′) Cu^I in $Ni_2Cu_4S_4$adam. Average bond distances and angles are given (with standard uncertainties in parentheses).

Figure 3. Ball-and-stick representation comparing the Cu_6S_4 core of Cu_6S_4adam and adamantane.

average dihedral angles $\angle S_2M$ and $\angle N_2M$ are 2.6° and 2.0°, respectively. The daco component maintains the N−M−N angle very close to 90° in each case, whereas the S−M−S angle is slightly more open in Cu_6S_4adam (averaging 94.9°) than in $Ni_2Cu_4S_4$adam (averaging 91.6°).

As is typical in copper thiolate clusters, the coordination about the Cu^I ions in Cu_6S_4adam and $Ni_2Cu_4S_4$adam is, with one exception, trigonal planar (Figure 2(a′) and 2(b′))), with S−Cu−S angles of ca. 110° and S−Cu−Cl angles of ca. 124° common to both clusters. A pyramidal distortion of one S_2Cu^ICl unit, with the Cu^I displaced out of the trigonal S_2Cl plane by 0.4 Å and toward the acetonitrile solvent molecule, is observed for one-half of the Cu_6S_4adam molecules. Although the Cu^I−NCMe distance of 2.567 Å is some 0.4−0.5 Å longer than bona fide Cu^I−NCMe bond distances in four-coordinate Cu^I complexes containing three soft (P or S) donor ligands,[20] the spatial orientation of the acetonitrile with respect to the Cu^I suggests a definite and specific long-range dipole−ion interaction.

Notably, the average Cu^{II}−S and Cu^I−S bond distances are statistically the same in Cu_6S_4adam. This is due to compensatory effects of the larger coordination number (which should increase the copper−sulfur distance) vs the increased charge (which should decrease the copper−sulfur distance) on the Cu^{II} relative to Cu^I. This phenomenon is seen in other mixed-valent copper thiolate clusters, as reported by Schugar and co-workers[21] and by Francesconi and co-workers.[22]

Figure 3 shows a ball-and-stick representation of $C_{10}H_{16}$ adamantane[23] alongside the Cu_6S_4 portion of Cu_6S_4adam. In

adamantane, the C−C distances average 1.536(5) Å and the C−C−C angles, 109.4(7)°.[23b] The average of all Cu−S distances in Cu_6S_4adam is 2.25(2) Å, and as listed in Table 2, there are five sets of angles about the adamantane-like core: Two are due to S−Cu−S and are 94.9(6)° ($\angle S−Cu^{II}−S$) and 108(2)° ($\angle S−Cu^I−S$); one is due to $Cu^I−S−Cu^I$ and averages 105°; and the remaining sets are $Cu^{II}−S−Cu^I$ and are ca. 100° and 130°, demonstrating distinct asymmetry in the two Cu_3S_3 fused cyclohexane rings that emanate from the N_2S_2Cu apex. The difference in the $Cu^{II}−S−Cu^I$ angles can be ascribed to the orientation of the mercaptoethyl portion of the bme*daco ligand (Figure 1 and Table 2) and the steric hindrance that the gem-dimethyl groups impose on the nearest Cu^I−Cl groups. Similar comparisons can be made between adamantane and $Ni_2Cu_4S_4$adam.

Analysis of the metal−metal distances within the $M_2Cu_4S_4$adam cavity finds the maximum to be the intra-cluster $Cu^{II}−Cu^{II}$ and $Ni^{II}−Ni^{II}$ distances of 5.43 and 5.54 Å, respectively, while the smallest, ca. 3.3 Å, is between the divalent cations and the nearest Cu^I projecting from the more open side of the $N_2S_2M^{II}$ plane. Such a cavity size would accommodate only the smallest molecule or atom.

Mass Spectral Data. Electron spray ionization mass spectra of the title compounds can be assigned on the basis of the rich isotopic pattern expected for polynuclear copper and nickel−copper clusters containing sulfur and chloride. Example spectra and full listings of these features, along with mass ranges and relative abundances, are given in the Supporting Information. Fragmentation and aggregation pathways that account for the major species are given in Scheme 2a and b for Cu_6S_4adam; Scheme 3a and b contains analogous results for $Ni_2Cu_4S_4$adam.

As sampled from acetonitrile solutions, the base peak of the all-copper complex is the two-electron-oxidized dication of the Cu_6S_4adam cluster with two acetonitrile solvent molecules bound to it ($m/z = 591.59$). Both higher- and lower-order clusters form the top five species, identified by numerical rankings in Scheme 2, with the dicationic parent cluster plus a CuCl second in abundance, 39.4%. This is the first in a series of dicationic aggregates of [Cu_6S_4adam· 2MeCN]$^{2+}$ that take up 1, 2, 3, and 4 CuCl molecules (Scheme 2a). In addition, the mass spectrum shows features corresponding to monocationic Cu_6S_4adam aggregates that have lost a chloride ion ($m/z = 1062.82$), leading into a degradative manifold with losses of (bme*daco)Cu as well

(20) *ConQuest*, version 1.4; Cambridge Crystallographic Data Centre: Cambridge, U.K., 2002.
(21) Bharadwaj, P. K.; John, E.; Xie, C.-L.; Zhang, D.; Hedrickson, D. N.; Potenza, J. A.; Schugar, H. J. *Inorg. Chem.* **1986**, *25*, 4541−4546.
(22) Sukal, S.; Bradshaw, J. E.; He, J.; Yap, G. P. A.; Rheingold, A. L.; Kung, H. F.; Francesconi, L. C. *Polyhedron* **1998**, *18*, 7−17.
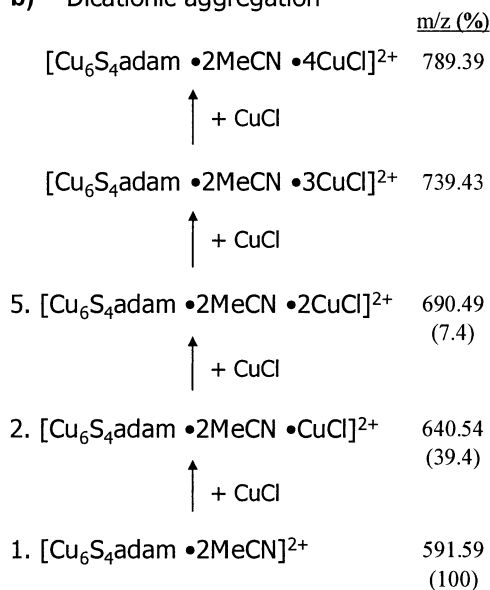(23) (a) Nordman C. E.; Schmitkons, D. L. *Acta Crystallogr.* **1965**, *18*, 764−767. (b) Donohue, J.; Goodman, S. H. *Acta Crystallogr.* **1967**, *22*, 352−354.
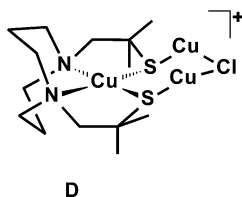
Scheme 2

a) Monocationic Aggregation/Degradation

$$Cu_8S_4Cl_5^+$$

$\uparrow$ + CuCl

$$Cu_7S_4Cl_4^+$$

$\uparrow$ + CuCl

$$[Cu_6S_4adam] - Cl^- \equiv Cu_6S_4Cl_3^+$$
m/z = 1064.7 (2.8 %)

-(bme*daco)Cu ↙   ↘ - CuCl

$$Cu_5S_2Cl_3^+$$ (3.9 %)

- CuCl ↙   ↘ - CuCl

4. $Cu_4S_2Cl_2^+$ (16.6 %) $Cu_4S_4Cl^+$

- CuCl ↙

3. $Cu_3S_2Cl^+$ (28.2 %)

b)   Dicationic aggregation

m/z (%)

$[Cu_6S_4adam •2MeCN •4CuCl]^{2+}$ 789.39

$\uparrow$ + CuCl

$[Cu_6S_4adam •2MeCN •3CuCl]^{2+}$ 739.43

$\uparrow$ + CuCl

5. $[Cu_6S_4adam •2MeCN •2CuCl]^{2+}$ 690.49
(7.4)

$\uparrow$ + CuCl

2. $[Cu_6S_4adam •2MeCN •CuCl]^{2+}$ 640.54
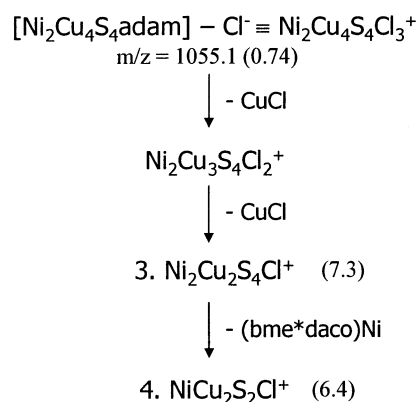(39.4)

$\uparrow$ + CuCl

1. $[Cu_6S_4adam •2MeCN]^{2+}$ 591.59
(100)
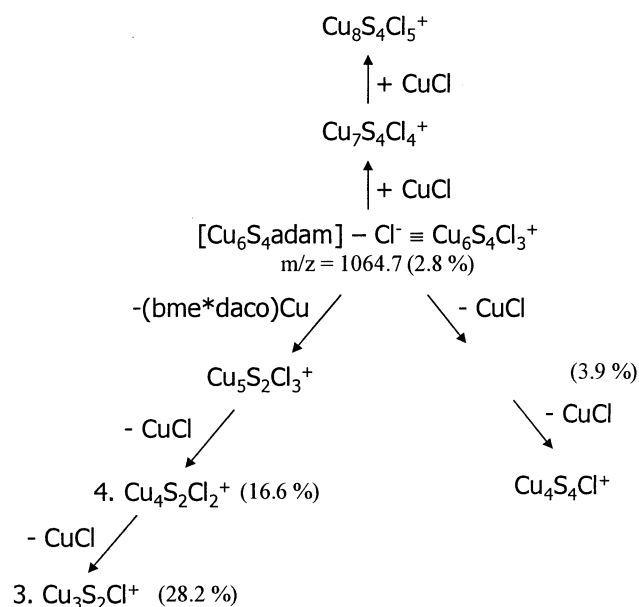
as, successively, two copper chloride moieties (Scheme 2b). The smallest cluster observed in the mass spectrum is an N_2S_2Cu complex with two additional Cu^I ions presumably bound to the sulfur atoms that is in relatively high abundance, 28.2%. A likely structure, **D**, is shown below.
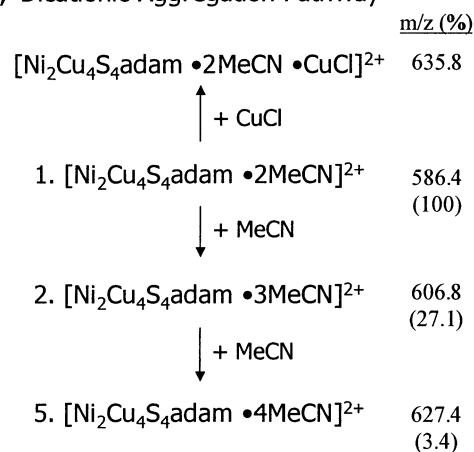

D

That the lower-order clusters might be isolable was demonstrated by a fortuitous choice of a crystal from a batch

Scheme 3

a) Monocationic Degradation Pathway

$$[Ni_2Cu_4S_4adam] - Cl^- \equiv Ni_2Cu_4S_4Cl_3^+$$
m/z = 1055.1 (0.74)

$\downarrow$ - CuCl

$$Ni_2Cu_3S_4Cl_2^+$$

$\downarrow$ - CuCl

3. $Ni_2Cu_2S_4Cl^+$ (7.3)

$\downarrow$ - (bme*daco)Ni

4. $NiCu_2S_2Cl^+$ (6.4)

b) Dicationic Aggregation Pathway

m/z (%)

$[Ni_2Cu_4S_4adam •2MeCN •CuCl]^{2+}$ 635.8

$\uparrow$ + CuCl

1. $[Ni_2Cu_4S_4adam •2MeCN]^{2+}$ 586.4
(100)

$\downarrow$ + MeCN

2. $[Ni_2Cu_4S_4adam •3MeCN]^{2+}$ 606.8
(27.1)

$\downarrow$ + MeCN

5. $[Ni_2Cu_4S_4adam •4MeCN]^{2+}$ 627.4
(3.4)

of decomposed (bme*daco)Cu. The source of the chloride in the isolated CuCl-deficient cluster is not known, and this synthesis has not been repeated. By X-ray crystallography, this compound was determined to be an aggregate containing five copper atoms, and three acetonitrile solvent molecules of crystallization, $[(bme*daco)Cu_2(\mu-CuCl)_3]•3MeCN$, a formulation related to the highlighted $Cu_5S_4Cl_2^+$ species in Scheme 2a. The X-ray crystal structure of this compound was solved in the monoclinic space group $P2_1/n$ with 4 molecules of the complex and 12 acetonitrile molecules in the unit cell. Inspection of the molecular structure shown in Figure 4 reveals one fewer CuCl moiety present as compared to four in Cu_6S_4adam, with only minor structural differences otherwise. The average bond distances and angles are similar to those found in Cu_6S_4adam. A full structural report is given in the Supporting Information.

The mass spectral data obtained for the $Ni_2Cu_4S_4adam$ cluster shows fewer components as compared to the all-copper analogue. Again, the base peak is assigned to a dicationic cluster with two acetonitrile molecules bound to it ($m/z = 586.4$). There are also features corresponding to the addition of three and four acetonitriles to the parent and of one copper chloride to the dicationic disolvated cluster. Again, a monocationic aggregate consisting of a single

Table 3. Physical, Spectroscopic, and Electrochemical Data for (bme*daco)Cu, Cu$_6$S$_4$adam, Ni$_2$Cu$_4$S$_4$adam, and (bme*daco)Ni

	(bme*daco)Cu	Cu$_6$S$_4$adam	(bme*daco)Ni	Ni$_2$Cu$_6$S$_4$adam
color	red	dark red	violet	orange
μ_{eff}, BM^a (20°C)	1.81	2.51	diamagnetic	diamagnetic
UV^b (nm (ϵ))^c				
LMCT	198 (9500)	206 (36 000)	−	234 (41 000)
	352 (6500)	454 (6300)		
d−d	504 (590)	−	350 (143)	−
			498 (90)	
cyclic voltammetry^d				
$E_{1/2}$ (V), (N$_2$S$_2$) M$^{II/I}$	−1.07	−0.63, −0.49	−2.12	−1.33
i_{pa}/i_{pc}	1.14	0.89	0.95	0.80

^{a} Measured in the solid state and by Evan's method at 20 °C. ^{b} Obtained using a 10-mm cell. ^{c} Units of M^{-1} cm^{-1}. ^{d} In CH$_3$CN solutions with concentrations of (bme*daco)Cu: 2.25mM, Cu$_6$S$_4$adam: 2.25 mM, and Ni$_2$Cu$_2$S$_4$adam: 1.13 mM and a glassy carbon as working electrode vs Ag/AgCl and TBAHFP as the supporting electrolyte with scan rate of 200 mV/s.
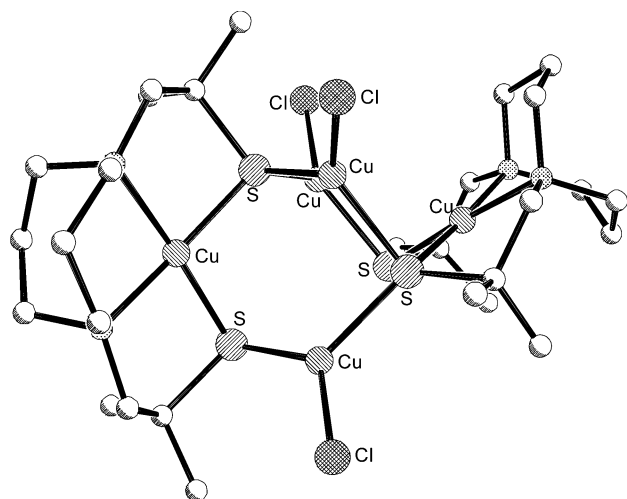
Figure 4. Ball-and-stick representation of the molecular structure of Cu$_5$S$_4$adam′ with selected atoms labeled. Hydrogen atoms are omitted.

Figure 5. Cyclic voltammagrams of (a) (bme*daco)Cu and (b) Cu$_6$S$_4$adam. TBAHFP (0.1 M) as the electrolyte in CH$_3$CN; scan rate of 200 mV/S. The concentrations of (bme*daco)Cu and Cu$_6$S$_4$adam were 2.25 mM.

(bme*daco)Ni with two copper(I) and one chloride ions bound to it, analogous to the N$_2$S$_2$Cu^{II}·Cu$^I_2$Cl structure **D** shown above, is present. A full listing of these features, all of which display the isotopic pattern expected for clusters containing several nickel, copper, chloride, and sulfur atoms, is given in Supporting Information.

Electrochemistry. A summary of electrochemical, electronic spectral, and magnetic susceptibility data is found in Table 3. The cyclic voltammogram, shown in Figure 5a, of (bme*daco)Cu in acetonitrile solution shows one reversible reduction wave centered at −1.07 V vs NHE, a quasireversible oxidation wave at +0.01 V, and a second irreversible oxidation event at ca. +0.55 V. The event at −1.07 V is assigned to the Cu$^{II/I}$ couple and is considerably more negative than that in monomeric N$_2$S$_2$Cu^{II} complexes where there is a ligand-imposed tetrahedral twist that better accommodates the reduced Cu^I d^{10} species.[24] For example, the reversible Cu$^{II/I}$ redox couple of the Schugar N$_2$S$_2$Cu^{II} complex, structure **C**, is −0.51 V vs NHE, measured in acetonitrile and referenced to Fc/Fc$^+$.[10] Its greater accessibility relative to (bme*daco)Cu can be ascribed to its distinct distortion toward tetrahedral symmetry, whereas (bme*daco)Cu is expected to be ligand-constrained to approximately square-planar geometry.[24]

(24) Knoblauch, S.; Hartl, F.; Stufkens, D. J.; Hennig, H. *Eur. J. Inorg. Chem.* **1999**, 303−312.

No oxidation event occurs between that for the −1.07 and 0.01 V waves, and the oxidation at 0.01 V is seen even without first scanning through the −1.07 reduction event. Because of these observations, it seems unlikely that the quasireversible oxidative event pertains to an altered species (as has been seen in other N$_2$S$_2$Cu^{II} complexes),[24] and therefore, we assign it to the Cu$^{III/II}$ redox couple of (bme*daco)Cu. The irreversible oxidation at ca. +0.55 V is attributed to S-ligand oxidation with subsequent irreversible chemical reaction.

The CV of Cu$_6$S$_4$adam shown in Figure 5b is only slightly more complicated than that of monomeric (bme*daco)Cu. A comparison finds the two redox events that were assigned to monomeric (bme*daco)Cu are shifted by ca. +0.5 V when this moiety is incorporated into the aggregate and each is resolved into two components. Two reversible Cu$^{II/I}$ reduction waves are centered at −0.63 and −0.49 V, and two Cu$^{III/II}$ couples are centered at +0.40 and +0.58 V; both are assigned to Cu within the N$_2$S$_2$ coordination sphere. The more positive Cu$^{II/I}$ reduction potentials and accompanying shifts in Cu$^{III/II}$ oxidation potentials find analogy in electro-

chemical studies of (bmedaco)Ni, (bme*daco)Ni, and S-metalated and S-oxygenated derivatives.[5,25,26] The stabilization of the $Ni^{II/I}$ redox couple in the latter compounds was ascribed to a decrease in the S-lone-pair−filled-Ni-d-orbital antibonding interaction that is present in the dithiolate complex upon the engagement of those lone pairs in bonding interactions. Such a change in ligand donor environment, which increases accessibility of the one-electron reduction process, concomitantly destabilizes the one-electron oxidation process, largely to the same extent.[25]

The resolution of each $Cu^{II/I}$ and $Cu^{III/II}$ into two events in the Cu_6S_4adam cluster complex implies electronic communication between the two copper(II) centers. Addition of the first electron to one $N_2S_2Cu^{II}$ unit influences the second. Thus, at least some electron delocalization exists in the cluster, presumably mediated via the d^{10} Cu^I−SR atoms through a sigma bond exchange pathway as there are no lone pairs on sulfur for ligand−metal charge transfer. Even the shortest Cu−Cu distance (3.3 Å) is beyond overlap possibility.

The cyclic voltammogram of $(Ph_2PCH_2CH_2PPh_2)CuCl$, (diphos)CuCl,[27] was recorded in MeCN to provide a reference point for any electrochemical activity involving the S_2Cu^ICl moiety of Cu_6S_4adam. Acetonitrile solutions of (diphos)CuCl showed an irreversible oxidative event at −0.4 V that shifted to −0.25 V with repeated scans. A similar phenomenon associated with the oxidation of Cu^I was clearly seen in the cyclic voltammogram of $Ni_2Cu_4S_4$adam; however this region of the cyclic voltammogram was open for the all-copper cluster. These observations were taken as evidence of greater delocalization in the latter as contrasted to the former. That is, the $N_2S_2Ni^{II}$ metallothiolate is a diphos mimic toward Cu^I, whereas the $N_2S_2Cu^{II}$ metallothiolate ligand permits orbital overlap with Cu^I that delocalizes the one-electron oxidized product. Results from electron spin resonance studies (vide infra) support this conclusion.

A broad reversible reduction event at −1.33 V in the CV of $Ni_2Cu_4S_4$adam is attributed to the $Ni^{II/I}$ couple in cluster-bound (bme*daco)Ni, and its singularity indicates localization of electron density on individual units within the cluster. Each unit is largely independent of the other, with little electronic communication between the two. Notably, the value of the $Ni^{II/I}$ couple is ca. 0.8 V more positive in the cluster than in the free (bme*daco)Ni, indicating the charge-neutralization effect of the S-bound CuCl units as was seen in earlier studies of the polymetallic aggregates shown in Chart 1.[5] Both the diminished electron-donating ability of the thiolates and the loss of the S-lone-pair−M_d antibonding interaction account for the increased accessibility of the $M^{II/I}$ redox couple. The observation of two irreversible oxidative events highly similar to those of (diphos)CuCl suggests that the metallothiolates have phosphine-like electron-donating abilities.

Electronic Spectra and Colors. The assembly of colorless CuCl and the colored N_2S_2M monomers into adamantane-like clusters results in distinct color differences. Acetonitrile solutions of (bme*daco)Cu are deep red; the Cu_6S_4adam cluster is intensely red-black, and its solutions are almost opaque to light. Electronic spectra are consistent with the qualitative observations. There are three bands in the vis/UV spectrum of (bme*daco)Cu: those at 198 nm ($\epsilon = 9500$ M^{-1} cm^{-1}) and 352 nm ($\epsilon = 7000$ M^{-1} cm^{-1}) are assigned to L → M charge-transfer bands, consistent with assignments made in the extensive study of Schugar et al.[10] A ligand field transition is observed at 504 nm (590 M^{-1} cm^{-1}). In the vis/UV spectrum of Cu_6S_4adam, two bands with much greater molar absorptivity coefficients are observed at 206 nm ($\epsilon = 36\,000$ M^{-1} cm^{-1}) and 454 nm ($\epsilon = 6300$ M^{-1} cm^{-1}).

More obvious color differences occur in the (bme*daco)-Ni/$Ni_2Cu_4S_4$adam pair. Violet MeCN solutions of (bme*daco)-Ni have LF or d−d electronic absorptions at 350 nm ($\epsilon = 143$ M^{-1} cm^{-1}) and at 498 nm ($\epsilon = 90$ M^{-1} cm^{-1}). A single band at 234 nm ($\epsilon = 41\,000$ M^{-1} cm^{-1}) is observed in the $Ni_2Cu_4S_4$adam electronic spectrum, and dilute solutions (ca. 0.1 mM) are yellow.

Detailed assignments of mixed-valence copper thiolate clusters have been initiated by Schugar et al., using a series of cluster complexes based on the N_2S_2Cu complex **C** with supporting documentation from circular dichroism spectroscopy.[10] Attempted assignments in our significantly different $Ni_2Cu_4S_4$ complexes would be, at this point, largely if not entirely speculative.

Magnetism/Electron Paramagnetic Resonance Spectroscopy. Whereas the $Ni_2Cu_4S_4$adam cluster is diamagnetic as expected, the magnetic moments of (bme*daco)Cu and Cu_6S_4adam, established by the Evan's method[13] in MeCN solution at 22 °C, are 1.81 and 2.51, respectively. Gouy balance measurements on the solids confirmed these values, which are consistent with one unpaired electron in the monomer and indicative of at least some coupling of spins from the two copper(II) ions in the cluster.

The X-band (9.05 GHz) EPR spectrum of (bme*daco)Cu as a 0.2 mM ethanolic glass at 8 K and 0.2 mW of power indicated anisotropy (Supporting Information), consistent with the odd electron in the d_{x2-y2} orbital of square-planar $N_2S_2Cu^{II}$, and simulated with the parameters $g_{||} = 2.118$, $g_\perp = 2.031$, $A_{||}^{Cu} = 182 \times 10^{-4}$ cm^{-1}, and $A_\perp^{Cu} = 49 \times 10^{-4}$ cm^{-1}. These values are similar to those obtained by Tolman and co-workers for (bmedaco)Cu[8a] and also for the tetrahedrally distorted $N_2S_2Cu^{II}$ square-planar complex **C**.[10] In contrast, the EPR spectrum of Cu_6S_4adam displays a broad isotropic signal centered at $g = 2.061$. A similar result was reported for a pentanuclear mixed-valent cluster comprising three $(N_2S_2)Cu^{II}$ units serving as bidentate bridging ligands to two Cu^I ions in a paddlewheel structure analogous to the $[(bmedaco)Ni]_3(ZnCl)_2^{2+}$ structure shown in Chart 1.[21] In that case, the conclusion of Schugar et al. was that weak ferromagnetic intracluster interactions between the Cu^{II} ions were transmitted via a S−Cu^I−S superexchange pathway.[21] Whether such an exchange pathway can exist in the Cu_6S_4adam cluster is not known. Unlike the Schugar et al. cluster, where the

(25) Farmer, P. J.; Reibenspies, J. H.; Lindahl, P. A.; Darensbourg, M. Y. *J. Am. Chem. Soc.* **1993**, *115*, 4665−4674.

(26) Buonomo, R. M.; Font, I.; Maguire, M. J.; Reibenspies, J. H.; Tuntulani, T.; Darensbourg, M. Y. *J. Am. Chem. Soc.* **1995**, *117*, 963−973.

(27) Marsich, N.; Camus, A.; Cebulec, E. *J. Inorg. Nucl. Chem.* **1972**, *34*, 933−946.

Cu^I ions are in a trigonal environment and where each S retains one lone pair,[21] the sulfurs in the Cu_6S_4adam cluster are fully valence-saturated. Nevertheless, the μ_B per Cu^{II} ion for the Cu_6S_4adam cluster (1.26 v_B Cu^{II}) is less than that for Schugar *et al.*'s Cu_5S_6 cluster (1.71 μ_B),[21] suggesting the existence of some coupling mechanism, perhaps via Cu to Cu.

Reactivity. To check for metal lability, specifically Cu^I, the cluster complexes were exposed to $Ph_2PCH_2CH_2PPh_2$, diphos, in tetrahydrofuran/acetonitrile mixtures. In the presence of 4 equiv of diphos a color change of the solution of Cu_6S_4adam indicated formation of (bme*daco)Cu. Simultaneously, a white precipitate was formed whose solubility characteristics matched those of an authentic sample of (diphos)CuCl (soluble in THF and insoluble in acetonitrile and methanol).[27] Under similar conditions, there was no reaction with $Ni_2Cu_4S_4$adam. This corroborates mass spectral data that indicate that the nickel-containing cluster is more stable than the all-copper cluster.

Conclusions

The nucleating ability of late-transition-metal, square-planar N_2S_2M complexes and the trigonal-planar coordination geometry preferences of Cu^I result in a highly regular adamantane-like structure for the $M_2Cu_4S_4$ clusters described above. The topology of these clusters results from the constrained conformation of the gem-dimethyl-derivatized bis-(*N,N*′-mercaptoethyl)-1,5-diazocyclooctane ligand that has previously provided a library of polynuclear structures. The symmetry in the $M_2Cu_4S_4$ structure, which is largely maintained in the $Cu_2^{II}Cu_3^IS_4$ cluster, is based on the approximately rigid square-planar (bme*daco) Cu template. A similar Cu_5S_4 complex based on the substantially distorted complex **C** adopts a cluster form with much less symmetrical or regular connectivity.[10] Although rare, the observation of a metal thiolate sulfur as a triply bridging ligand is not entirely uncommon in mixed-valent Cu^{II}/Cu^I complexes[10] and hence must be viewed as a possibility in polynuclear, mixed-valent copper thiolates as might be present in biological systems.

It is noted that the engagement of all sulfur lone pairs of (bmedaco)Ni in strong covalent bonding interactions via the formation of the nickel−sulfur oxygenate, the 1,5-bis(2-sulfino-2-methylpropyl)-1,5-diazocyclooctane complex of nickel, also results in a color change from violet to orange-yellow, whereas formation of the trimetallic of Chart 1, which leaves one lone pair on each S, generates a deep red-black species.[27]

Although their structural forms are the same, there are subtle and interesting differences in Cu_6S_4adam and $Ni_2Cu_4S_4$adam, arising from distinctions in their magnetic, electronic, electrochemical, and chemical properties. That CuCl can be removed by the chelate diphos ligand from the Cu_6S_4adam but not the $Ni_2Cu_4S_4$adam cluster supports our previous characterization of (bme*daco)Ni as a metallo-thiolate ligand with S-donor properties similar to those of thioethers or phosphines.[5,7,25] Indeed, from the recent report of such a bonding motif as $N_2S_2Ni−Cu^I$ in a metalloenzyme that performs transformations associated with organometallic chemical catalysis,[28] we are tempted to conclude that the metallothiolate has been enlisted by nature as a soft ligand to facilitate low-valent chemistry. Thiolate-bridged bimetallics in enzyme active sites might therefore be considered as single-site metal centers, capable of classical organometallic reactivity and redox changes as might occur in phosphinated transition metal complexes.

Supporting Information Available: Complete details (CIF format) of the X-ray diffraction studies for compounds Cu_6S_4adam, $Ni_2Cu_4S_4$adam, and Cu_5S_4adam′ with extended packing diagrams. Listings of metal−metal distances, mass spectral data. Figures of mass spectral isotopic patterns, EPR spectra of (bme*daco)Cu and Cu_6S_4adam, and CVs of $Ni_2Cu_4S_4$adam and (diphos)CuCl. This material is available free of charge via the Internet at http://pubs.acs.org.

IC0262684

(28) Doukov, T. L.; Iverson, T. M.; Seravalli, J.; Ragsdale, S. W.; Drennan, C. L. *Science* **2002**, *298*, 567−572.